

I.D. Stolyarchuk¹, G.I. Kleto², A. Dziedzic³

Structural and optical properties of Co and Ni doped ZnO thin films prepared by RF magnetron sputtering

¹Ivan Franko Drohobych Pedagogical University, 24 I. Franko str., 82100 Drohobych, Ukraine, e-mail: istolyarchuk@ukr.net

²Chernivtsi National University, 2 Kotsyubynsky Street, 58012 Chernivtsi, Ukraine,

³Centre for Innovation and Transfer of Natural Sciences and Engineering Knowledge, University of Rzeszow, 16, a Rejtana Street, 35959 Rzeszow, Poland, e-mail: dziedzic@univ.rzeszow.pl

We have reported the effect of Co and Ni doping on structural and optical properties of ZnO thin films prepared by RF reactive sputtering technique. The composite targets were formed by mixing and pressing of ZnO, Mn₃O₄, CoO and NiO powders. The thin films were deposited on sapphire, quartz and glass substrates. The structure study confirms the formation of the hexagonal wurtzite ZnO without any secondary phase in transition metal (Co, Ni) - doped samples. Cross-sectional TEM images of all studied samples show a dense and uniformly textured structure composed of column-like structure along the growth direction. The surface morphology of the thin films was studied using atomic force microscopy (AFM). Different surface morphology (AFM) images were obtained depending on the film composition and growth conditions. Optical absorption spectra suggest substitution Zn²⁺ ions in ZnO lattice by transition metal atoms. The shift of the absorption edge due to decrease the energy band gap with increasing cobalt content and complex dependence of the energy band gap on content of nickel was observed in optical absorption spectra of the studied films. The room temperature photoluminescence peaks are attributed to near band gap emission and vacancy or defect states.

Keywords: diluted magnetic semiconductor, zinc oxide, thin films, rf sputtering, X-ray diffraction, transmission electron microscopy, atomic force microscopy, optical absorption, photoluminescence.

Стаття постулила до редакції 11.08.2017; прийнята до друку 05.09.2017.

Introduction

Diluted magnetic semiconductors (DMS) are attractive materials because of exhibition of the sp-d exchange interaction between the localized magnetic moments and the spins of the band carriers. The replacement of the cations of III-V or II-VI nonmagnetic semiconductors by magnetic transition metals (TM) ions leads to a number of magnetic, optical, magneto-optical and magnetotransport phenomena. The unique spin-dependent phenomena in these semiconductors can introduce new functionality to spintronic devices. Recently the family of DMSs was increased by addition of the semiconducting oxides [1, 2].

Zinc oxide (ZnO), an optically transparent II-VI semiconductor with hexagonal wurtzite structure of C_{6v}⁴ (P6_{3mc}) space group, wide direct band gap (E_g ~ 3.37 eV), excitons binding energy (~ 60 meV) has been identified as a promising host material after theoretical studies have predicted ferromagnetism above room temperature in Mn-doped ZnO [3]. Different growth techniques such as chemical vapor deposition, spray

pyrolysis, pulsed laser deposition, magnetron sputtering, sol-gel process etc have been used for preparing of ZnO-based DMSs thin films. Several groups [4-7] have observed ferromagnetism in ZnO:TM systems, while other groups [8-10] have not observed such magnetic behavior in similar samples. These controversial results indicated that the magnetic properties are very sensitive to the shape of the samples and to the preparation conditions.

The present work is devoted to preparing of Co or Ni doped ZnO thin films and study of their structural and optical properties depending on content of transition metals.

I. Experimental

The films of Zn_{1-x}Co_xO and Zn_{1-x}Ni_xO were prepared by RF reactive sputtering technique. Glass, quartz and sapphire were used as the substrates. Mixture of argon and oxygen was used as the reactive gases. The distance from target to substrate was taken as 35 mm. The details

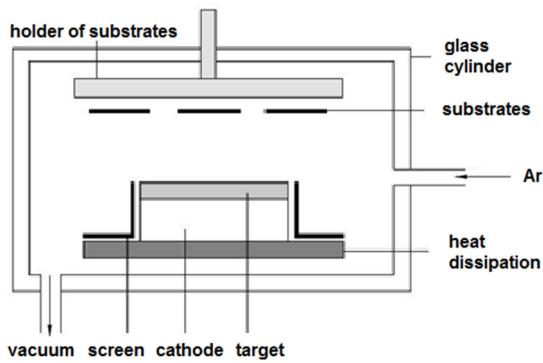


Fig. 1. Scheme of the deposition experiment.

of the target-substrate experimental setup are shown in Fig. 1. The base vacuum in the chamber was $2 \cdot 10^{-4}$ Pa and the working gas pressure – 0.2 Pa of oxygen and 0.8 Pa of argon. Sputtering was carried out with input RF power 300 W and deposition rate of 10 nm/min. Post deposition annealing (5-8) min in oxygen atmosphere at (500 - 550) $^{\circ}$ C was performed.

Targets were prepared by pressing with using of ZnO, Mn_3O_4 , CoO and NiO pure powders as initial components. The temperature of substrates were 350 - 400 $^{\circ}$ C during deposition process and was measured by two chromel-copel thermocouples, which were placed on the back side of the substrate holder.

The crystallographic studies were performed using X-ray Diffractometer (D8 ADVANCE X-ray Diffractometer with DAVINCI) using Cu- K_{α} wavelength ($\lambda = 1.54059 \text{ \AA}$) and scanning in 2θ range from 10° to 70° . A Tecnai Osiris X-FEG S/TEM microscope was used for recording high-resolution (HR) TEM images. Atomic force microscopy (AFM) was used to evaluate the surface morphology of the films. The sample of $Zn_{1-x}Mn_xO$ was measured in Semicontact Mode with standard NT-MDT NSG03 (Resonance Frequency

$F = 90 \text{ KHz}$, Force Constant $K = 1.74$). The samples of $Zn_{1-x}Co_xO$ and $Zn_{1-x}Ni_xO$ also was measured in Dynamic Mode (non-contact) with Force constant $K \sim 40 \text{ N/m}$ and $f_0 \sim 300 \text{ kHz}$.

Absorption spectra between 350 and 600 nm were measured using a grating monochromator, a photodetector system and registered computer system. This setup has also served to register photoluminescence (PL) spectra. For such kind of measurements the samples were excited using a 325 nm He-Cd laser with an excitation intensity value of 10 mW.

II. Results and Discussion

The obtained XRD patterns of the pure ZnO and $Zn_{1-x}Me_xO$ (Me- Co, Ni) oxides showed that all as-grown samples are nanostructured polycrystalline films. The diffraction patterns of all samples can be indexed to the hexagonal wurtzite structure of ZnO. The X-ray diffraction (XRD) patterns of $Zn_{0.96}Ni_{0.04}O$ films on glass and sapphire substrates are shown in Fig. 2. All intense peaks positions of the films correspond to the standard diffraction pattern of ZnO hexagonal wurtzite with a (002) preferred orientation. No peaks corresponding to TM clusters or their oxides are observed on the patterns which indicates that Co or Ni has entered the ZnO lattice without changing the wurtzite structures and systematically substituted the Zn^{2+} ions in the lattice. The relative intensity of the (002) peak of the $Zn_{1-x}Co_xO$ and $Zn_{1-x}Ni_xO$ ($0 \leq x \leq 0.08$) exhibits stronger than other peaks, indicating that the C-axis preferred texture growth of the TM-doped ZnO films. Further, the intensity of diffraction peaks of thin films increased with increasing TM concentration which can be attributed to a refinement and improvement of crystalline quality of these films as a result of Co or Ni doping. At same time, we observed shift only in the angular peak position of (002) plane and no angular shift was observed for any other plane. This angular peak shift towards the lower 2θ value from the undoped sample to doping of $x = 0.04$

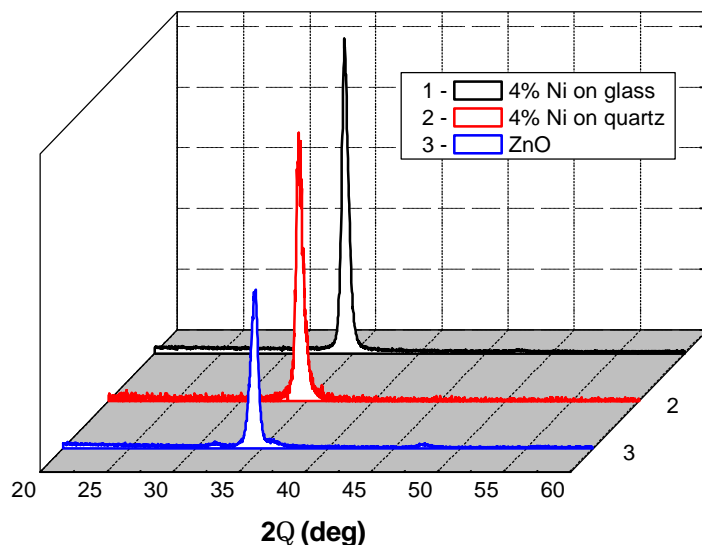


Fig. 2. X-ray diffraction spectra of $Zn_{1-x}Ni_xO$ thin films on glass and sapphire substrates.

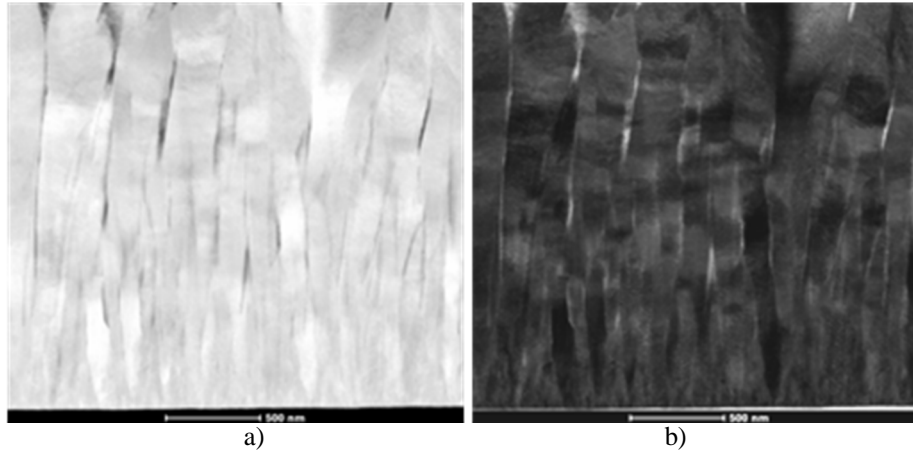


Fig. 3. STEM HAADF (Z – kontrast) (a) and STEM BF (b) images of $Zn_{1-x}Co_xO$ thin films.

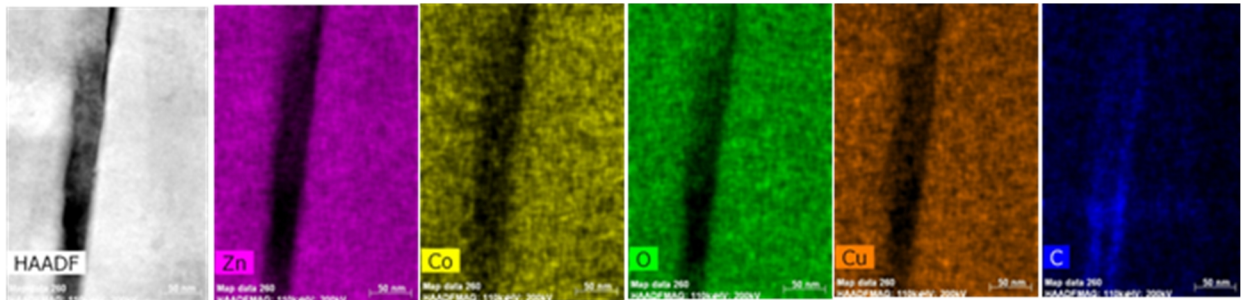


Fig. 4. The EDX maps showing of chemical elements in selected area.

indicates that films are in a uniform state of stress. With a further increase in TM concentration, the peak shift takes place in opposite direction, i.e. 2θ value increased, indicating the change in the direction of stress. The average crystallite size, D was calculated using the full width at the half maximum (FWHM) of the diffraction peak and the angle of diffraction θ in Debye-Scherrer's formula [11]:

$$D = \frac{0,9 \lambda}{\Delta\theta \cos \theta}, \quad (1)$$

where λ is the X-ray wavelength, $\Delta\theta$ is the FWHM and θ is the Bragg angle of the diffraction peak. Analyzing the obtained results, a decrease of crystallite size with increasing TM dopant concentration is observed. It seems that the introduction of Co(Ni) atoms in ZnO structure and increasing their concentration slightly reduces the average crystallite size. The same behavior was reported for ZnO:Ni [12] and ZnO:Al thin films [13]. The authors consider that some quantity of dopant atoms prefers to locate in or near the grain boundary regions, determining a decrease of crystallite size. TM-doped slightly decreased the lattice parameters of the ZnO films, considering that the size of Co^{2+} (0.058 nm) and Ni^{2+} (0.055 nm) in tetrahedral configuration is close to the size of Zn^{2+} in tetrahedral coordination (0.06 nm). Thus, the Co^{2+} or Ni^{2+} ions were systematically substituted by Zn^{2+} ions without changing the crystal structure.

Cross-sectional transmission electron microscopy (TEM) images of all studied samples show a dense and uniformly textured structure composed of column-like structure along the growth direction (Fig. 3). The corresponding selected-area the energy dispersive X-ray

detection (EDX) maps are shown in Fig. 4. All the locations contain the expected elements (Zn, Co, O) and no other impurity elements apart from Cu and C (from grid), clearly indicating that Co is uniformly distributed in the film and makes solid solution with ZnO matrix.

The surface morphology of the $Zn_{1-x}Me_xO$ films and their crystallite sizes have been studied and evaluated by AFM. The obtained results suggest that the values analyzed by AFM are much higher than the ones analyzed by XRD. As well known, with AFM the size is measured by the distance between the visible grain boundaries, which is called particle size. While with XRD, the grain size is measured in the extent of crystalline region that the diffract X-ray, which is more stringent and leads to smaller size. The surface morphology of the layers studied by AFM shows strong dependence on oxide composition, substrate material and growth conditions. The root mean square of the surface roughness is measured from the pictures over $2 \mu m \times 2 \mu m$ and $5 \mu m \times 5 \mu m$ scanning range. The AFM micrograph shown in Fig. 5, a indicates that the increase in the surface roughness by Co doping is caused by closely packed nanorod like nanocrystallites throughout the $Zn_{0,98}Co_{0,02}O$ film surface. The estimated diameter of the observed nanorods is about 100 nm. Essentially, there is no obvious change in the microstructure observed in the films grown with different Co concentrations. The surface morphology of the $Zn_{1-x}Ni_xO$ film shows a mixture of granular and columnar microstructures (Fig. 5, b). The average roughness R_{ms} of these films was 65.7 nm, and the average grain size was 62.5 nm. Similar AFM images with columnar microstructures were observed recently in $Zn_{1-x}Ni_xO$ films prepared by DC

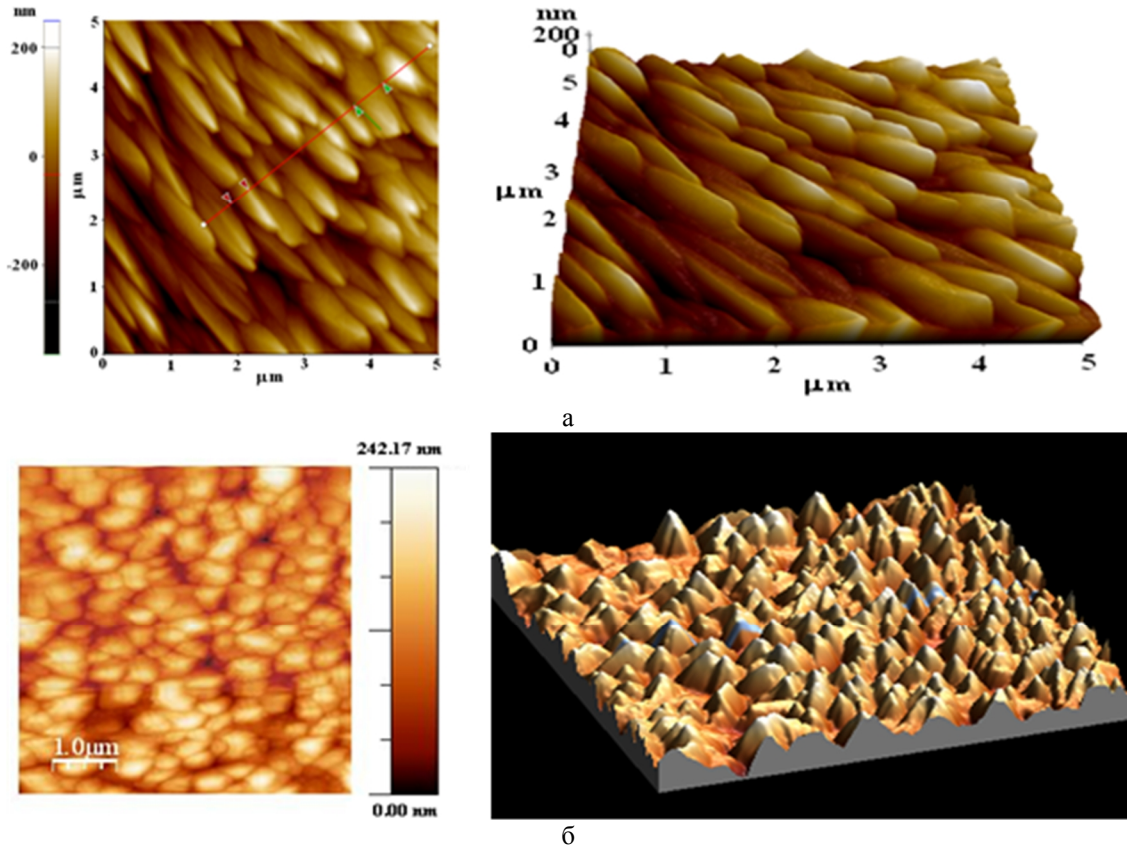


Fig. 5. 2D and 3D AFM images of thin films: (a) $Zn_{0.98}Co_{0.02}O$ on glass substrate, (b) $Zn_{0.98}Ni_{0.02}O$ on glass substrate.

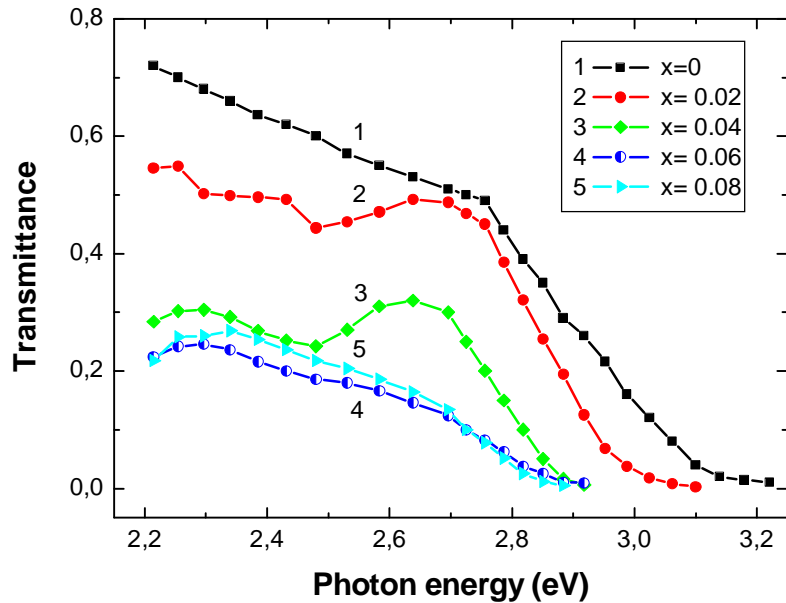


Fig. 6. Transmittance spectra of $Zn_{1-x}Co_xO$ thin films with different content of Co in spectral region near the absorption edge.

magnetron sputtering [14] and sol-gel spin coating method [15]. It should be noted that the difference between AFM images for Co-doped and Ni-doped ZnO films is that nanorods in the first case are closed packed and tilted whereas for the second case columns are oriented perpendicularly to film substrate plane.

UV-Vis optical measurements were carried out at room temperature to study the effect of TM (Co, Ni) doping concentration on the band gap of ZnO thin films

and to confirm the substitution of Co^{2+} or Ni^{2+} ions in tetrahedral sites of the ZnO wurtzite structures. Fig. 6 shows the optical transmission spectra of undoped and cobalt doped ZnO thin films deposited on glass substrates. The undoped ZnO film is more transparent whereas in cobalt doped thin films the transmittance decreases with the increase of Co-doping concentration. The optical transmittance spectra showed a shift in the band edge towards lower energy side with the increase of

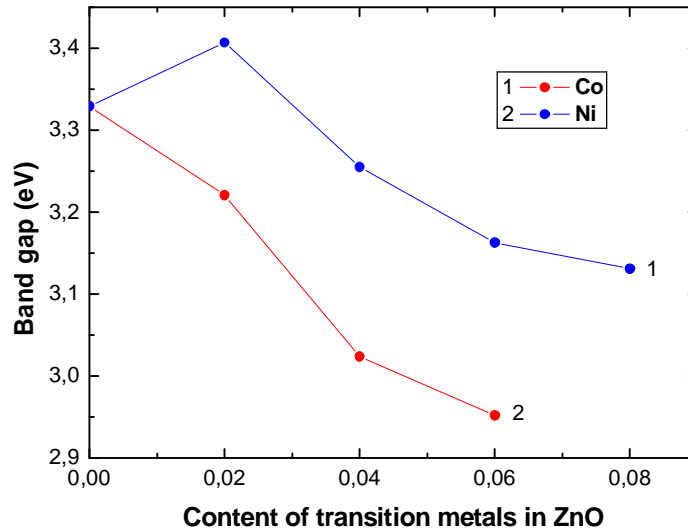


Fig. 7. The energy band gap of TM doped ZnO thin films as a function of Co and Ni- content.

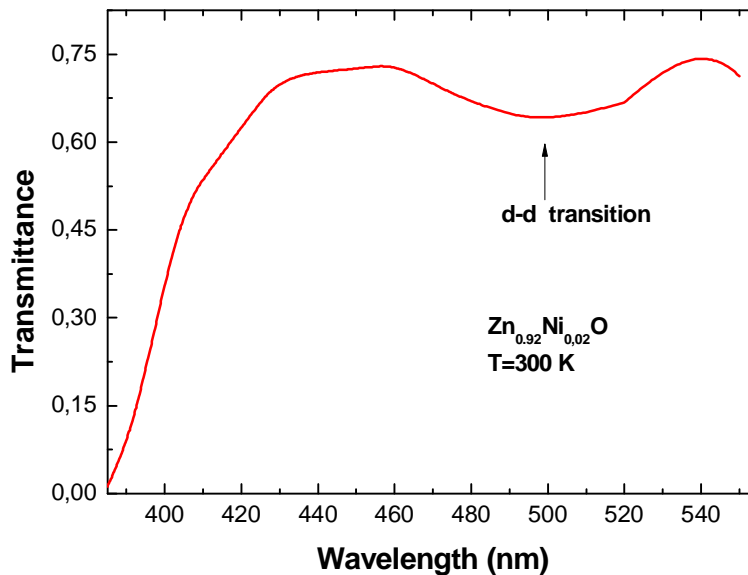


Fig. 8. Transmittance spectrum of $Zn_{0.98}Ni_{0.02}O$ thin film in spectral region corresponding d-d transitions.

Co content in the films. Additional absorption below the absorption edge can be seen for the $Zn_{1-x}Co_xO$ thin films. In particular, for Co content of $x = 0.02$ three absorption bands at about 1.87, 2.03 and 2.19 eV have been revealed, which are in agreement with already reported absorption peaks [16, 17]. This absorption structure is associated with d-d electron transitions of Co^{2+} ions in a tetragonal crystal field. The observed peaks were attributed to ${}^4A_1(F) \rightarrow {}^2A_1(G)$, ${}^4A_2(F) \rightarrow {}^4T_1(P)$ and ${}^4A_2(F) \rightarrow {}^2E(G)$ transitions in Co^{2+} ions. The observation of these transitions in transmission spectra of our $Zn_{1-x}Co_xO$ films, thus, clearly reveals that the added cobalt atoms have been substituted by Zn^{2+} cations and are present in 2+ state.

The band gap E_g of the $Zn_{1-x}Co_xO$ films have been calculated using plotting of $(\alpha h\nu)^2$ versus $h\nu$ and by extrapolating the linear portion of the absorption edge to find the intercept with energy axis. The estimated of E_g values are decreased with increase of Co content (Fig. 7). This result is in contrast with the reported data [16, 18],

where blue shift of the absorption edge was observed. On the other side, a similar trend of decrease of band edge in $Zn_{1-x}Co_xO$ films is reported by many workers [5, 17, 19]. This low energy shift of the E_g as a function of the Co content can be explained due to the s,p-d exchange interactions between the band electrons and the localized d electrons of the Co^{2+} ions substituting for Zn^{2+} ions [20, 21]. The s-p and p-d exchange interactions give rise to a negative and a positive correction to the conduction and valence-band edges, leading to narrowing of the band gap [22].

Compared with pure ZnO film, both for the $Zn_{1-x}Co_xO$ films, the optical absorption edge of $Zn_{1-x}Ni_xO$ films is shifted depending on content of Ni. Upon Ni doping, the absorption edge is blue shifted for $x \leq 0.02$ and red shifted for the films with $x > 0.02$. The estimated values of E_g are increased with increase of Ni content up to $x = 0.02$ and decreased for $x > 0.02$ (Fig. 7). This result is in contrast with the reported data [14, 23], where only red shift of the absorption edge was observed. Such

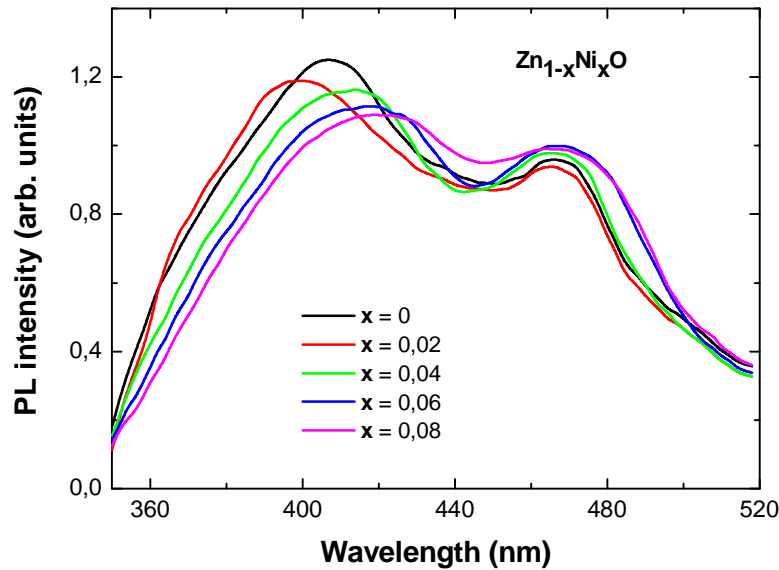


Fig. 9. The PL spectra of $Zn_{1-x}Ni_xO$ films with different Ni-content.

a kind of $E_g(x)$ dependence might be due to the formation of defect energy level of Ni. As a donor impurity, Zn_i produces a shallow donor levels, which can reduce the band gap of ZnO. According to recent suggestion of Reddy et al. [23] decrease of E_g with increase of Ni-content for the sprayed thin films can be associated with the structural defects such as voids and dangling bonds that can also create the localized states in the band gap. More complex character of absorption edge dependence, but very similar to the our thin films was reported for $Zn_{1-x}Ni_xO$ nanoclusters prepared by co-precipitation method [24]. Because of the nanostructured character of the prepared $Zn_{1-x}Ni_xO$ films according to the demonstrated above AFM images the same mechanism can be applied also to explain the observed dependence.

Both for the $Zn_{1-x}Co_xO$ thin films, additional absorption below the absorption edge can be seen for the $Zn_{1-x}Ni_xO$ films. To observe this feature we have chosen for measurements more thicker film as compared with thickness of the films for analysis of the absorption edge. From Fig. 8 we can see in transmittance spectrum of $Zn_{0.98}Ni_{0.02}O$ film wide absorption band around 480 - 520 nm. This absorption structure is associated with d-d electron transitions of Ni^{2+} ions in a tetragonal crystal field. In particular, the observed peak can be attributed to ${}^3T_1(F) \rightarrow {}^3T_1(P)$ transitions of the Ni^{2+} ions.

The PL spectra of $Zn_{1-x}Ni_xO$ films with different Ni-content are shown in Fig. 9. All the spectra contain a strong emission band at 380 nm, which is due to free excitonic recombination or electron transitions from the conduction band to the valence band of ZnO. The energy position of this band is shifted to lower photon energy with increase of Ni – content in accordance with the reducing of the band gap. The PL peak at 460 nm is due to different vacancies and defect states. The intensity of this band increases with increase of Ni – content. Gao et al. [14] discussed possible influence of six intrinsic

defects such as antisite oxygen, antisite zinc, oxygen vacancy, zinc vacancy, interstitial oxygen and interstitial zinc.

Conclusions

In conclusion, $Zn_{1-x}Co_xO$ and $Zn_{1-x}Ni_xO$ thin films with $x \leq 0.08$ were deposited by RF reactive sputtering technique on sapphire, glass and quartz substrates. XRD analysis of the films reveal that cobalt or nickel ions are successfully doped in ZnO without changing the hexagonal wurtzite structure. The grown TM doped ZnO films show c-axis preferred orientation with good crystallinity. The $Zn_{1-x}Co_xO$ film is composed of closely packed nanocrystallites with nanorod shape and $Zn_{1-x}Ni_xO$ film shows a mixture of granular and columnar microstructures.

The optical absorption spectra of the films demonstrate: (a) the energy band gap was found to decrease with Co content increase, (b) the absorption edge is found to be shifted in different manner depending on Ni-content, (c) the presence of d-d transitions. These observations conclusively prove that in studied films Co and Ni exist in $2+$ states at tetrahedral sites and substitutes Zn^{2+} . The room temperature photoluminescence peaks were revealed for all samples and are attributed to near band gap emission and vacancy or defect states.

Stolyarchuk I.D. - PHD of physics and mathematics, associate professor, professor of the department of physics;

Kleto G.I. - researcher, department of semiconductor physics and nanostructures;

Dziedzic A. - PhD of Physics and Mathematics.

- [1] S. J. Pearton, W.H. Heo, M. Ivill, D.P. Norton, T. Steiner, *Semicond. Sci. Technol.* 19, R59 (2004).
- [2] S. J. Pearton, D.P. Norton, K. Ip, W.H. Heo, T. Steiner, *Prog. Mater. Sci.* 50, 293 (2005).
- [3] T. Dietl, H. Ohno, F. Matsukura, J. Cibert, D. Ferrand, *Science* 287, 1019 (2000).
- [4] P. Sharma, A. Gupta, F.J. Owens, A. Inoue, K.V. Rao, *J. Magn. Magn. Mater.* 282, 115 (2004).
- [5] K. P. Bhatti, V. K. Malik, S. Chaudhary, *J. Mater. Sci: Mater. Electron* 19, 849 (2008).
- [6] C. Liu, B. Xiao, F. Yun, H. Lee, U. Ozgur, Y.T. Moon, H. Morkoc, M. Abouzaid, P. Ruterana, *Superlattices Microstruct.* 39, 124 (2006).
- [7] E. Liu, P. Xiao, J.S. Chen, B.C. Lim, L. Li, *Current Appl. Phys.* 8, 408 (2008).
- [8] T. Fukumura, Z. Jin, M. Kawasaki, T. Shono, T. Hasegawa, S. Koshihara, H. Koinuma, *Appl. Phys. Lett.* 78, 958 (2001).
- [9] Y. Belghazi, M. AitAouaj, M. El Yadari, G. Schmerber, C. Ulhaq-Bouillet, C. Leuvrey, S. Colis, M. Abd-lefdil, A. Berrada, A. Dinia, *Microelectr. J.* 40, 265 (2009).
- [10] A.S. Risbud, N.A. Spaldin, Z.Q. Chen, S. Stemmer, and R. Seshadri, *Phys. Rev. B* 68, 205202 (2003).
- [11] B.D. Cullity, *Elements of X-ray diffractions*, Addison-Wesley, Reading, 1978.
- [12] A.P. Rambu, L. Ursu, N. Iftimie, V. Nica, M. Dobromir, F. Iacomi, *Applied Surface Science* 280, 598 (2013).
- [13] S. Venkatachalam, Y. Iida, Y. Kanno, *Superlattices and Microstructures* 44, 127 (2008).
- [14] F. Gao, L.X. Tan, Z.H. Wu, X.Y. Liu, *J. Alloys Compd.* 484, 489 (2009).
- [15] R. Siddheswaran, R.V. Mangalaraja, E. P. Tijerina, J.-L. Menchaca, M.F. Melendrez, R.E. Avila, C. E. Jeayanthi, M.E. Gomez, *Spectrochim. Acta A*, 106, 118 (2013).
- [16] J.H. Kim, H. Kim, D. Kim, S.G. Yoon, W.K. Choo, *Solid State. Commun.* 131, 677 (2004).
- [17] K.J. Kim, Y.R. Park, *Appl. Phys. Lett.* 81 (8), 1420 (2002).
- [18] [M. Subramanian, M. Tanemura, T. Hihara, V. Ganesan, T. Soga, T. Jimbo, *Chem. Phys. Lett.* 487, 97 (2010).
- [19] S. Colis, H. Bieber, S. Begin-Colin, G. Schmerber, C. Leuvrey, A. Dinia, *Chem. Phys. Lett.* 422, 529 (2006).
- [20] L. Wei, Z. Li, W.F. Zhang, *Appl. Surf. Science* 255, 4992 (2009).
- [21] X. Xu, C. Cao, *J. Alloys Compd.* 501, 265 (2010).
- [22] J.K. Furdyna, *Diluted magnetic semiconductors*, *J. Appl. Phys.* 64 (4), R29-R67 (1988).
- [23] M.R. Reddy, M. Sugiyama, K.T.R. Reddy, *Adv. Mater. Res.* 602-604, 1423 (2013).
- [24] R. Gopalakrishnan, S. Muthukumar, *J. Mater. Sci: Mater. Electron.* 24, 1069 (2013).

I.Д. Столярчук, Г. І. Клето, А. Дзедіч

Структурні та оптичні властивості тонких плівок ZnO, легованих Co та Ni, отриманих методом іонно-плазмового напилення

¹Дрогобицький педагогічний університет ім. Івана Франка, вул. І.Франка, 24, 82100 Дрогобич, Україна, e-mail: istolyarchuk@ukr.net

²Чернівецький національний університет, вул. Коцюбинського, 2, 58012 Чернівці, Україна,

³Центр інновацій та передачі природних наук та інженерних знань, Жешувський університет, вул. Рейтана, 16, 35959, м. Жешув, Польща, e-mail: dziedzic@univ.rzeszow.pl

В роботі представлено результати експериментального дослідження структурних та оптичних властивостей тонких плівок ZnO, легованих Co та Ni, отриманих методом іонно-плазмового напилення. Композиційні мішені отримувались шляхом змішування та пресування порошкоподібних оксидів ZnO, Mn₃O₄, CoO та NiO. Тонкі плівки осаджувались на кварцевих, сапфірових та скляних підкладках. Отримані результати структурних досліджень свідчать про ріст плівок в гексагональній вюрцитній структурі з переважною орієнтацією (002) без утворення вторинних фаз. ТЕМ зображення поперечного перерізу всіх досліджених зразків свідчать про щільну наностержневу будову плівок вздовж напрямку зростання. Результати атомарно-силової мікроскопії демонструють складну морфологію поверхонь отриманих плівок, яка залежить від компонентного складу та умов їх одержання. В спектрах поглинання виявлено зменшення ширини забороненої зони плівок із зростанням вмісту кобальту та складну її залежність при зростанні вмісту нікелю. У спектрах фотолумінесценції при кімнатній температурі для всіх досліджуваних плівок виявлено смуги випромінювання, що відповідають екситонним переходам поблизу краю фундаментального поглинання та наявним домішкам і дефектам.

Ключові слова: магніторозчинений напівпровідник, оксид цинку, тонка плівка, іонно - плазмове напилення, X – променева дифракція, трансмісійна електронна мікроскопія, атомарно – силова мікроскопія, поглинання, фотолумінесценція.